

## Vectorization of human pelvis objects in X-ray images

**Algimantas Juozapavičius, Ramūnas Markauskas**

Faculty of Mathematics and Informatics of Vilnius University

Naugarduko str. 24, LT-03225 Vilnius, Lithuania

algimantas.juozapavicius@mif.vu.lt; ramunas.markauskas@mif.vu.lt

**Received:** 20 January 2011 / **Revised:** 14 April 2011 / **Published online:** 30 May 2011

**Abstract.** In medical diagnostics visual evaluation of an object or its image is necessary but time consuming operation. Well-known computer vision algorithms or their compilation, or even some new methods should be the right tool in increasing the speed and reliability of this process. This paper introduces situation in this domain and some experiments and their results in extraction of biomechanical parameters of human pelvis from x-ray images using combination of Hough transform for a line, for a circle (arc) and Canny edge detector. The main idea of an algorithm, which was created during this experiment, is to use different levels of noise filter thus making a balance between leaving too much noise and removing too much actual data. The basic steps would be: filter out most of noise and noisy objects using high filter's threshold value; find sharp and clear objects; narrow the set of possible parameters of noisy objects; apply noise filter with lower threshold value to the original image; find noisy objects. Experiment shows that algorithm works but it needs to be tested on reliability and some bindings with actual biomechanical parameters should be done (see [1–6]).

**Keywords:** Hough transform, human pelvis, biomechanical parameters.

### 1 Introduction

Contemporary medical diagnostics explores intensively visual evaluation of medical images, signals or other complicated objects. In some cases visual diagnostics is relatively simple (for example, in case of non-complicated bone fracture), however, in many other cases mere visual inspection is not sufficient and detailed diagnosis requires complex measurements, as well as extraction of biomechanical parameters of an object. The extraction of biomechanical parameters is a time-consuming process often prone to mistakes. One of the ways to reduce costs of this process and increase its reliability is to use computer vision algorithms, which can accelerate and unify the process, thus leaving to a physician just a function of interpretation, i.e. assessment of a medical condition, selection of an appropriate treatment method and evaluation of its efficiency. Different dysfunctions of an acetabulofemoral joint which result in pain and/or motility restrictions are important factors determining a person's quality of life. Such dysfunction may be congenital, caused by trauma or joint operation conditions (such as long-term joint strain

exceeding joint stress limits due to obesity, hard physical work, uncomfortable body position or repeated movements), natural wear on joints or may be a result of other pathologies. Around 10% of patients over 85 years of age suffer from a degenerative acetabulofemoral joint disease and according to the data of different studies, the occurrence of congenital joint dislocation among newborns due to insufficient development ranges from 3% to 7.5% of all cases. Modern medicine can help all patients suffering from these types of joint dysfunctions, however, treatment resources are not sufficient. Establishment of pathological diagnoses in the pelvic area (such as dysplasia, arthrosis, dislocation or fracture) and selection of treatment methods relies on a number of methods based on calculations involving biomechanical parameters of objects under analysis. These parameters can be conveyed in geometrical expressions: points, distances among objects, positions of objects to each other and angle formations. Currently all measurements are made manually using a protractor ruler or vector graphics applications. In general, the diagnostic process involves the following steps (see [4, 7]):

1. Pain diagnostics;
2. Anamnesis;
3. Patient examination (temperature, visual changes, palpation, pace, stand, movement extent);
4. Radiology test and extraction of biomechanical parameters;
5. Additional diagnostic methods, if necessary (computed tomography, radioisotope bone scan, ultrasound testing, magnetic resonance imaging, arthroscopy).



Fig. 1. Size of original x-ray and scanned image.

This, however, does not mean the end of the process – in order to evaluate the efficiency of the applied treatment method and joint replacement parameters, it is most often repeated several times. Therefore, more accurate primary diagnostics and systematic accumulation of experience would contribute to a more efficient performance of the entire system. This article presents experimental methodology for testing possibilities to

develop automatic tools used for extraction of biomechanical parameters in the diagnostic process. There are a number of medical methods for extracting biomechanical parameters. Some methods are used in primary diagnostics, certain calculations are made when observing the course of treatment, while other methods are employed only in exceptional cases when standard methods fail to provide enough information. The article presents a simulation of an automatic analysis of an x-ray image aimed at extracting different objects of a human structure, such as bone structures, the parameterisation of which would allow calculating biomechanical parameters used in the most commonly applied standard diagnostic methods. Moreover, the research has also produced a method for digitising x-ray images with the use of available means.

## 2 Digitisation of x-ray images

The main obstacle for digitisation of x-ray images is that in contrast to paper objects, x-ray images are relatively transparent, therefore, they reflect a smaller quantity of light emitted by scanning equipment and are less visible to an optical device of a scanner. The idea of the new method is to use an additional source of light thus making an x-ray image better recognisable to an optical device of a conventional scanner. X-rays of the pelvic bone area of an adult are usually done using two size formats:  $350 \times 350$  mm and  $350 \times 430$  mm. Each of these formats exceeds maximum sizes of originals accepted by a scanner by at least one dimension but objects under analysis fit within scanner dimensions, thus, at the expense of margins of the original image we retain relevant data. The steps of the scanning process are as follows: at first, a radiograph is placed on the scanner glass and covered with a sheet of paper which serves as a filter for even distribution of light and reduction of noises in the digitized image. Then, an additional source of light is prepared, switched on and scanning is started. During scanning, the original scanner equipment moves along the object being scanned and the operator follows its movement with the additional source of light and illuminates the spot being scanned. Digital images obtained using this method show real images of a radiograph and thus can be used for further analysis.

## 3 Research object

Objects under analysis are x-ray images of human pelvic bone area. The aim of the research is to separate objects which could be linked with biomechanical parameters or used as a basis for their calculation. Some possible links among objects and biomechanical parameters are presented in Table 1 (see [4]).

Table 1. X-ray objects and biomechanical parameters.

Object	Biomechanical parameter
Femoral ridges	Direction of a femur, femoral axis, femoral thickness, position of femurs to each other
Femoral head	Centre of the head, distance of the head from the femoral axis
Pelvic arches	Angle between the arches, angle between pelvic bones and femurs

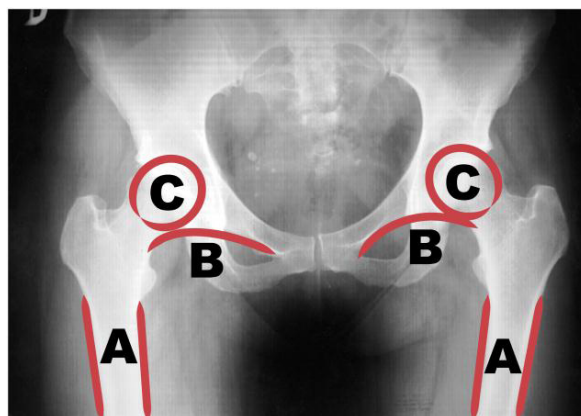


Fig. 2. A – femoral ridges; B – pelvic arches; C – femoral heads.

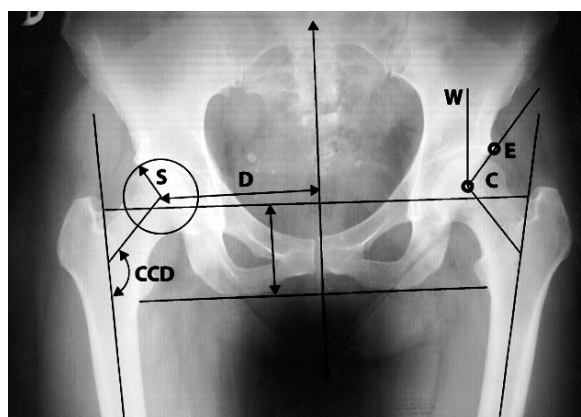


Fig. 3. Point E – upper acetabular edge; point C – centre of a femoral head; distance D – distance between the vertical body axis and centre of a femoral head; distance S – radius of a femoral head; angle CCD – angle between femoral neck and diaphysis.

#### 4 Methods

Object separation process may be divided in two stages: filtration of a primary image in order to remove excess data (such as visible fibres or inner bone structures) and object separation. At first the image is processed using a Gaussian convolution filter which smooths the image and then the Canny edge detection algorithm is applied to detect edges (two sets of parameters are used: a smaller filter helps to detect the most distinctive objects, whereas a larger filter leaves more noise and also more data about the objects under analysis). The Hough transform for straight lines is used to detect the most distinctive

objects, such as femur edges, whereas the Hough transform for circles, i.e. the Hough transform for curves, is used to find femoral heads and pelvic arches.

## 5 Object separation

**Step 1.** Smoothing of an original image. For this purpose the Gaussian convolution filter is used (experimentally chosen mask is shown in the Fig. 4);

$$\frac{1}{159} \begin{bmatrix} 2 & 4 & 5 & 4 & 2 \\ 4 & 9 & 12 & 9 & 4 \\ 5 & 12 & 15 & 12 & 5 \\ 4 & 9 & 12 & 9 & 4 \\ 2 & 4 & 5 & 4 & 2 \end{bmatrix}$$

Fig. 4. Experimentally chosen Gaussian convolution filter mask.

**Step 2.** Use of Sobel operator (the masks used are shown in the Fig. 5);

$$G_x = \begin{bmatrix} 1 & 2 & 1 \\ 0 & 0 & 0 \\ -1 & -2 & -1 \end{bmatrix} \quad G_y = \begin{bmatrix} -1 & 0 & 1 \\ -2 & 0 & 2 \\ -1 & 0 & 1 \end{bmatrix}$$

(a) X-axis mask                      (b) Y-axis mask

Fig. 5. Masks used with Sobel operator.

Given gradients of  $x$  and  $y$  directions the common gradient of a point is calculated by fewer operations using the formula  $|G| = |G_x| + |G_y|$ . However, when using this formula instead of the standard formula  $G = \sqrt{G_x^2 + G_y^2}$ , it is necessary to verify whether the gradient does not cross the boundaries of the interval of possible values, i.e. (1) where  $G_{min}$  and  $G_{max}$  is an interval of possible values of the gradient. This step helps to expose edge formations in a smoothed image.

$$\begin{cases} \text{if } |G| < G_{min}, & \text{then } G = G_{min}, \\ \text{if } |G| > G_{max}, & \text{then } G = G_{max}. \end{cases} \quad (1)$$

**Step 3.** Edge thinning. Given gradients of a point, the angle of an edge direction is calculated using the formula (2).

$$\alpha = \begin{cases} 0^\circ & \text{if } G_x = 0 \text{ and } G_y = 0, \\ 180^\circ & \text{if } G_x = 0 \text{ and } G_y \neq 0, \\ \arctan\left(\frac{G_x}{G_y}\right) & \text{otherwise.} \end{cases} \quad (2)$$

If  $G < G_\alpha$ , then  $G = 0$ , where  $G_\alpha$  is a value of the gradient of a point in direction  $\alpha$ . Finally, the thinned edges are linked applying two experimentally chosen thresholds  $T_{min} = 40$  and  $T_{max} = 240$  (see [8–12]). When searching for objects that are hard to distinguish, different threshold values will be used in order to leave more noise and also more data about the objects under analysis.

$$T = \begin{cases} 0 & \text{if } T < T_{min}, \\ T_{max} & \text{if } T > T_{max}, \\ T_{max} & \text{if } T_{min} < T < T_{max} \text{ and } T_{neighbor} \in E_{edgepoints}. \end{cases} \quad (3)$$

Point (3) is recognised as an edge pixel only in case it is adjacent to the pixel which is already the edge pixel or which is greater than  $T_{max}$ . This step helps to avoid separation of an edge into a set of smaller components. The Fig. 6 shows the processed radiographic image obtained by thinning and linking of edges.

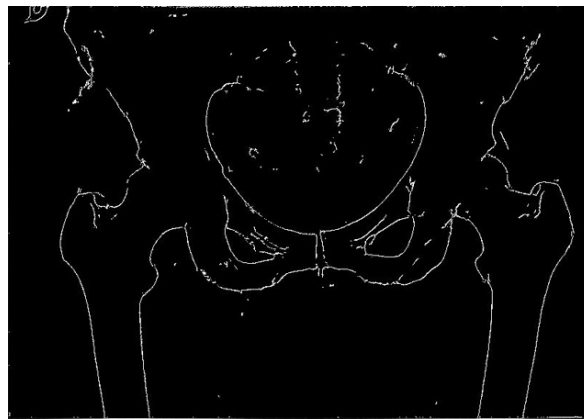


Fig. 6. Canny edge detector with  $T_{min} = 40$ .

**Step 4.** Detection of femoral ridges. When detecting straight lines in polar coordinates using the Hough transform and equation of a straight line  $r = x \cos \alpha + y \sin \alpha$ , it is necessary to set thresholds, since:

1. If no thresholds are set, all straight lines will be detected according to the same parameters, i.e. most probably in the same place where is the largest number of pixels constituting a line;
2. If the minimum threshold is set, i.e. that both parameters  $r_l$  and  $\alpha_l$  of a newly detected line  $l$  cannot be equal to parameters  $r_{l_o}$  and  $\alpha_{l_o}$  of any other detected line  $l_o$ , it will be impossible to avoid concentration of objects in the region of the most probable line, since one line in the image will be matched by a number of lines detected using the Hough transform, differences between parameters of which will be minimal.

Since none of the discussed variants are satisfactory, the following thresholds will be set for each newly detected line  $l$  with parameters  $r_l$  and  $\alpha_l$  and for a previously detected line  $l_o$  with parameters  $r_{l_o}$  and  $\alpha_{l_o}$ : a line is recognised as suitable only if  $|r_{l_o} - r_l| > \varepsilon_r$  and  $|\alpha_{l_o} - \alpha_l| \geq \varepsilon_\alpha$ , where  $\varepsilon_r$  is a value chosen with respect to the search area, in this case the dimensions of an original radiograph, and  $\varepsilon_\alpha$  may be equal to zero. The result obtained after carrying out the search using parameters  $\alpha$  ( $0^\circ \leq \alpha \leq 360^\circ$ ),  $\varepsilon_r = 50$ ,  $\varepsilon_\alpha = 0$  are shown in the Fig. 7. Due to femur qualities, the interval of the parameter  $\alpha$ , within which the lines are searched, may be reduced thus optimising the search. Having set the threshold  $-20^\circ < \alpha < 20^\circ$ , we obtain the same results as shown in the figure.

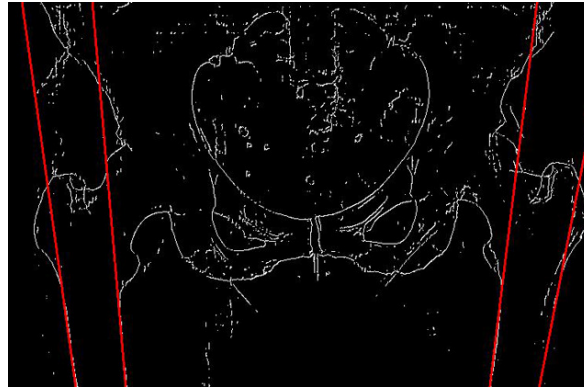


Fig. 7. Detected femoral ridges.

**Step 5.** Specification and detection of parameters of pelvic arches. Using the Hough transform (see [13, 14]) for circles and on the basis of already defined width and position of femurs as well as given interdependence of positions of objects to each other, the following parameters of an equation are defined:

1.  $r_{min} = Width_{femur} < r_{pelvicbonecurve} < \frac{3}{2} Width_{femur} = r_{max}$ ;
2. The search region is defined by a rectangle, the coordinates of the bottom left point of which are equal to the coordinates of the peak point of the segment of the inner femoral ridge, whereas width and height are defined by triple width of the femur;
3. Possible coordinates of the centre are defined in the area which expands to all directions from the search region by  $r_{max}$ ;
4.  $\alpha_{min}^{curve} = \alpha_{ridge} - 90^\circ$  and  $\alpha_{max}^{curve} = \alpha_{ridge} + 90^\circ$ .

After defining possible values of parameters, the detection of pelvic bone curves is performed.

**Step 6.** Specification of parameters of femoral heads. Femoral heads are described by the same equation as pelvic arches and assessment of their parameters is an equally important

task. However, as in the case described above, these parameters can be set only taking into account data about the already detected objects, i.e. data about the femoral and pelvic arches:

1.  $r_{min} = 0,55 * Width_{femur} < r_{head} < 0,65 * Width_{femur} = r_{max}$ ;
2. The search region is defined by a rectangle, the coordinates of the bottom left angle of which are equal to the centre of the pelvic arch, whereas width and height are equal to  $r_{max}$ ;
3. Coordinates of a possible centre are defined in the above search region;
4.  $\alpha_{min}^{curve} = \frac{9}{2} * \frac{\alpha_{inneridge} + \alpha_{outeridge}}{2}$ ,  $\alpha_{max}^{curve} = \frac{9}{2} * \frac{\alpha_{inneridge} + \alpha_{outeridge}}{2} + 190^\circ$ .

**Step 7.** Use of larger filter by applying Canny edge detector. Specification of possible parameters of femoral heads and their search in a given filtered image will not produce the desired result since the image does not contain enough information allowing to separate femoral heads. In order to solve this problem, the radiograph will be repeatedly filtered. The same parameters will be set for the Gaussian convolution filter and the Sobel operator but the threshold  $T_{min}$  used for edge linking will be changed from  $T_{min} = 40$  to  $T_{min} = 20$  thus giving the step of edge linking more degrees of freedom (result is shown in Fig. 8).



Fig. 8. Canny edge detector with  $T_{min} = 20$ .

**Step 8.** Recognition of femoral heads. The results show that the obtained image contains considerably more noise but it also provides sufficient information for recognition of femoral heads. Due to excess information, use of this set of points would not allow to separate precisely even the most distinctive objects but on the basis of information about them obtained by previous calculations we have assessed parameters of the objects that are hard to separate thus making them recognisable. Fig. 9 shows the separated objects, whereas Fig. 10 shows the same objects in the original x-ray image.



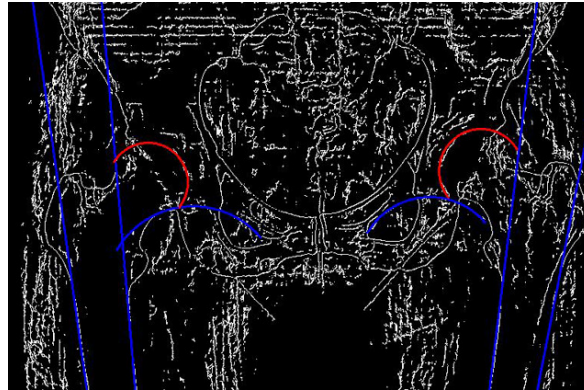


Fig. 9. Separated objects.

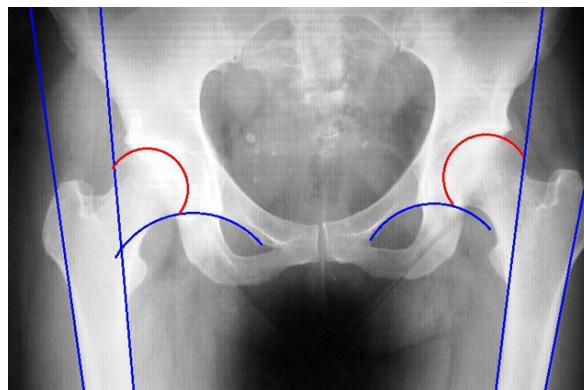


Fig. 10. Separated objects in original x-ray image.

## 6 Conclusions

In order to separate the required objects, a number of methods have to be applied when analysing radiographs. The most easily recognisable objects are femurs. They are detected by filtering the image applying the Canny edge detection algorithm and fragmenting the image using the Hough transform for straight lines (with certain thresholds set for four lines describing femoral ridges). When searching for clearly visible pelvic arches we have to set additional thresholds for parameters due to peculiarities of the equation describing pelvic arches and the radiograph itself (besides pelvic arches the image also contains other curvy objects). This is done on the basis of the data about the detected femoral ridges. After defining the parameters pelvic bones are successfully detected. Previous calculations and parameters of detected objects allow describing parameters of femoral heads but due to lack of information the search is repeatedly carried out using the

Canny edge detection algorithm with more degrees of freedom in the filtered radiograph (schema of an algorithm is shown in Fig. 11).

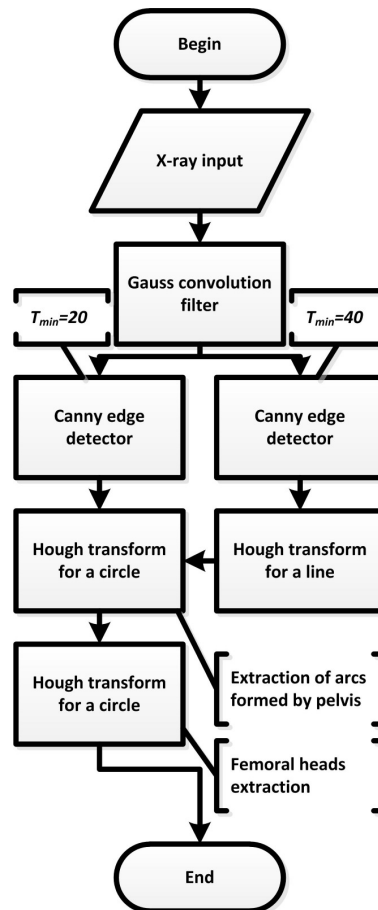


Fig. 11. Schema of an algorithm.

These methods can be successfully applied when detecting distinctive femurs and pelvic bones as well as femoral heads that are hard to distinguish. Without separation of femurs in the first stage, the methods described above would not allow to process images, since other detection steps rely on the information about femurs. In order to avoid this problem, after the first stage of detection data can be submitted to a user for evaluation of their accuracy. If the user is not satisfied with the results, he/she can narrow the search region, specify intervals of other parameters and carry out a repeated search. Having obtained the desired accuracy of the data, the user can allow the application to take further steps of detection.

## 7 Further research

In further stages the researcher plans to:

1. Specify a set of recognisable objects and calculate/separate biomechanical parameters;
2. Examine the adaptability of the developed methods for diagnostics of other body areas which is based on the analysis of bone structures visible in x-ray images;
3. Examine the adaptability of the developed methods for diagnostics of other areas which is based on the visual analysis of objects in 3D images.

## References

1. N. L. Frederiksen, Diagnostic imaging in dental implantology, *Oral Surg. Oral Med. O.*, **80**(5), pp. 540–554, 1995.
2. D. Manning, Evaluation of diagnostic performance in radiography, *Radiography*, **4**(1), pp. 49–60, 1998.
3. C. J. Martin, P. F. Sharp, D. G. Sutton, Measurement of image quality in diagnostic radiology. *Appl. Radiat. Isotopes*, **50**(1), pp. 21–38, 1999.
4. N. Porvaneckas, *Total Hip Arthroplasty*, Vilnius Univ. Press, Vilnius, 2008 (in Lithuanian).
5. M. D. Sewell, K. Rosendahl, D. M. Eastwood, Developmental dysplasia of the hip, *Brit. Med. J.*, **339**(7732), pp. 1242–1248, 2009.
6. P. Suetens, E. Bellon, D. Vandermeulen, M. Smet, G. Marchal, J. Nuyts, L. Mortelmans, Image segmentation: methods and applications in diagnostic radiology and nuclear medicine, *Eur. J. Radiol.*, **17**(1), pp. 14–21, 1993.
7. N. Porvaneckas, G. Kvederas. Hip biomechanics assessment before and after replacement surgery. *Medicina*, **35**, pp. 1212–1220, 1999 (in Lithuanian).
8. L. Ding, A. Goshtasby, On the canny edge detector, *Pattern Recognition*, **34**(3), pp. 721–725, 2001.
9. M. A. Fischler, O. Firchein, *Readings in Computer Vision: Issues, Problems, Principles, and Paradigms*, Morgan Kaufmann Publishers Inc., 1987.
10. M. Heath, S. Sarkar, T. Sanocki, K. Bowyer, Comparison of edge detectors: a methodology and initial study, *Comput. Vis. Image Und.*, **69**(1), pp. 38–54, 1998.
11. M. Sharifi, M. Fathy, M. Mahmoudi, A classified and comparative study of edge detection algorithms, in: *Proceedings of the International Conference on Information Technology: Coding and Computing*, IEEE Computer Society Washington, DC, USA, pp. 117–120, 2002.
12. R. Wang, *Canny Edge Detection*, 2004.
13. D. Ballard, Generalizing the hough transform to detect arbitrary shapes, *Pattern Recognition*, **13**(2), pp. 111–122, 1981.
14. J. Illingworth, J. Kittler, A survey of the hough transform, *Computer Vision, Graphics, and Image Processing*, **44**(1), pp. 87–116, 1988.